Enhancement of sum frequency generation near the photonic band gap edge under the quasiphase matching conditions

A. V. Balakin, V. A. Bushuev, B. I. Mantsyzov,* I. A. Ozheredov, E. V. Petrov, and A. P. Shkurinov
Department of Physics and International Laser Center, M. V. Lomonosov Moscow State University, Moscow, 119899, Russia

P. Masselin and G. Mouret
Laboratoire de PhysicoChimie de l'Atmosphère, CNRS EP 1831, Université du Littoral, 145 avenue Maurice Schumann, 59140, Dunkerque, France

(Received 8 September 2000; published 27 March 2001)

We analyze theoretically and study experimentally the mechanisms of enhancement of the sum frequency and second harmonic generation in a finite one-dimensional photonic band gap structure with second order nonlinearity under Bragg diffraction conditions. It is shown that, near the photonic band gap edge, the efficiency of conversion in sum frequency and second harmonic generation processes can be significantly enhanced if two conditions are fulfilled simultaneously: grating assisted phase matching, or quasiphase matching, and an increase of the electromagnetic field density at the fundamental frequencies near the photonic band edges. The role of each mechanism is discussed.

DOI: 10.1103/PhysRevE.63.046609 PACS number(s): 42.70.Qs, 42.65.−k, 42.79.Nv

I. INTRODUCTION

The problem of the development and optimization of frequency converters of laser radiation has existed since the beginning of the laser era [1,2]. To have sufficient efficiency of conversion of the light wave frequency (multiplication, mixing, etc.), a material (usually the crystalline one) must satisfy two basic requirements. First, noticeable nonlinear optical effects can be observed only when the light propagates through a fairly long crystal and the so-called ''phase matching conditions'' are fulfilled. In this case the generated nonlinear optical field propagates through the media in phase with the field at the fundamental frequency (FF) [2]. Second, the material should be noncentrosymmetric in order to have a second order nonlinear optical response [3] and to allow the source of nonlinear optical polarization. In the optical transparency region in isotropic media (and also in anisotropic crystals for waves of identical polarization), under normal dispersion conditions phase matching can never be fulfilled. Thus we have to conclude that phase matching conditions are fulfilled only in anisotropic crystals with differently polarized waves [2,3].

In addition to the material requirements to increase the conversion efficiency in the nonlinear optical process, the density of the field at the FF inside the nonlinear optical material has to be increased. In practice, the amplitudes of the fields at the FF are set as a constant along the length of interaction, and this is true in the bulk of the nonlinear optical crystal in the planar wave approximation.

Consequently, in the case of ''typical'' crystalline materials we are quite limited in the choice of measures for the optimization of the conversion efficiency. The usual way is mainly concerned with a search for materials with the largest nonlinear coefficients, that rarely can be fitted well with phase matching conditions. The optimization of the field distribution inside the nonlinear optical material is not typically used.

This problem may be solved absolutely unexpectedly in the periodically modulated materials that have been under intensive study by the optical community during the last decade. These materials are called photonic crystals (PC's) [4,5]. Such PC structures present spatially periodic modulations of their dielectric functions (linear refractive index and/or nonlinear optical susceptibility). The spatial period of modulation has a dimension close to the wavelength of light. In the case of low modulation of the refractive index, under the assumption of linear light-matter interaction, light propagation in PC's is similar to Bragg diffraction of x rays in traditional crystals [6]. Particular interest is concerned with studies of artificial structures with a high contrast of the refractive index modulation ($\Delta n \sim 1-2$) and/or with a consideration of the nonlinear interaction of light with PC's. This led to the discovery of new physical effects such as the existence of complete photonic band gaps (PBG's), i.e., frequency ranges where the propagation of light in the case of linear interaction is forbidden inside the structure [5]. Following this the possibility of light localization [7] and spontaneous emission control [8], as well as the existence of optical Bragg solitons in the area of complete linear PBG's [9], were studied. Moreover, in nonlinear PC's the behavior of the selective Bragg scattering has its own specific properties for achieving phase matching conditions, as compared with linear PC's [10,11].

The study of nonlinear optical phenomena in one-dimensional PC's with periodic modulations of linear and nonlinear susceptibilities [12], has been the focus of attention since the pioneering publications of Bloembergen and coworkers [13], where a new mechanism of phase matching that takes into account the reciprocal lattice vector of periodic media was suggested. Following the terminology of a review paper [12], the grating assisted phase matching is called ''quasiphase matching'' if there is a periodic distribu-

*Email address: mants@genphys.phys.msu.su

tion of nonlinear susceptibility only; it is called ''linear'' quasiphase matching if there is a periodic modulation of the linear refractive index, but the nonlinear susceptibility is space independent. In both cases the physical reason for the phase matching condition is the same: the reciprocal lattice vector of nonlinear or linear structures is included in phase matching conditions for wave vectors of fields. The structure studied in the present paper has a periodic modulation of both linear and nonlinear susceptibilities with equal spatial periods. Thus here we shall use the term quasiphase matching (QPM) in its generalized meaning in order to delineate that the phase matching is fulfilled due to the reciprocal lattice vector but not due to the dispersive mechanism. Phase matching conditions can also be satisfied due to the ''traditional'' dispersive mechanism near the PBG's because of the essential change (both increasing and decreasing) of the effective refraction index of the composite media [14]. In addition to these phase matching mechanisms to increase the efficiency of the nonlinear optical process, there is a nonphase matching one, concerned with increasing the energy density of the field inside the structure when the frequency of the fundamental field is tuned near the PBG edge. This mechanism was recently described theoretically [15,16] and studied experimentally [17] for multilayer structures with deep modulations of the refractive index. In Ref. [15] the possibility of increasing the intensity of the second harmonic (SH) signal in a PBG structure because of a nonphase matching enhancement mechanism, and at the same time the satisfaction of the conditions of dispersive phase matching, was theoretically shown. In Ref. [18] we described and experimentally studied the effect of a nonphase matching enhancement of the intensity of the signal at the sum frequency (SF) in the PBG structure under conditions of simultaneously increasing the density fields of both fundamental frequencies near the opposite sides of the PBG.

One of the interesting questions in studies of nonlinear optical phenomena in dielectric multilayer PC structures is the source of nonlinear optical polarization in each dielectric layer. In this paper we do not pay attention to this particular question. We only suppose that the source of nonlinear polarization exists in layers with a high refraction index—''nonlinear layers.'' The existence of this source is due to several main reasons. First, the origin of the nonlinear polarization comes from the crystalline or ordered nature of the material [2,3]. Second, in layers made of isotropic materials, the source of the nonlinear optical response may also exist. For instance, in Ref. [11] the nonlinear optical response arose from the chiral property of material. Another possibility to have a nonlinear optical response in the layers of isotropic material was proposed in Ref. [19], where the authors took into account the distortion of the wave function in inhomogeneous optical fields that appear naturally in multilayer periodic structures with a modulation of the refraction index and/or of the nonlinear susceptibility. It is also well known that due to a breaking of the symmetry, second order processes may occur at the interface between two media [20].

In the present paper, we demonstrate theoretically and experimentally the possibility of the optimization of the efficiency of SH and SF generation due to the action of both QPM and nonphase matching simultaneously. The theoretical description is carried out on the basis of recurrence relations that allow one to obtain exact and complete solution of this problem for a nonlinear multilayer structure of finite length. The recurrence relation method, described in Sec. II, seems to us simpler and more convenient for a simulation of the nonlinear optical conversion in PBG multilayer structures compared with the traditionally used propagation matrix technique [21]. In Sec. III we theoretically study SF and SH generation in multilayer structure with a deep periodic modulation of linear ($\Delta n \sim 1$) and nonlinear susceptibilities. It is shown that due to the nonphase matching enhancement, the intensities of SF and SH signals under the condition of QPM interaction may be increased more than by one order of magnitude. Note that, in the case of the SH generation process, in addition to the exact fulfillment of the QPM condition, the phase matching caused by the dispersive properties of the PBG may also give a contribution to the intensity of the signal. This happens because at specific angles of incidence the edges of linear reflection curves at fundamental and SH frequencies are crossed. In Sec. IV we describe our experimental technique and the investigated sample. In Sec. V we show and discuss the experimental results on SF and SH generation in a ZnS/SrF_2 multilayer structure. In experiments we have obtained a nonphase matching enhancement of both the SF signal near the QPM condition and the SH signal under QPM interaction near dispersive phase matching conditions. The experimental data demonstrate good agreement with the theoretical predictions.

II. RECURRENCE RELATION METHOD

Let us consider the generation of a signal at a sum frequency $\omega_3=\omega_1+\omega_2$ in a multilayer structure (MS) by two incident planar monochromatic waves $\boldsymbol{E}_{1,2}^{(+)}$ at frequencies ω_1 and ω_2 and with the amplitudes A_1 and A_2,

$$\boldsymbol{E}_j^{(+)}(\boldsymbol{r},t)=\boldsymbol{e}_j^{(+)}A_j \exp[\,i(k_{jx}x+k_{jz}z)-i\omega_j t], \qquad (1)$$

where

$$k_{jx}=k_j \sin\vartheta_j, \quad k_{jz}=k_j\cos\vartheta_j, \quad k_j=\omega_j/c=2\pi/\lambda_j .$$

Here λ_j are the wavelengths of incident fields in vacuum, c is the light velocity in vacuum, $\boldsymbol{e}_j^{(+)}$ are the polarization vectors, and ϑ_j are the angles of incidence of corresponding waves. The direction of the z axis is taken as a positive into the MS, and the x axis is directed along the structure surface in the plane of incidence (x,z) (Fig. 1). A theoretical description is made for the general case, when the frequencies ω_1 and ω_2 and the angles ϑ_1 and ϑ_2 are different. For the particular case of collinear second harmonic generation $\omega_3=2\omega_1$, $\omega_1=\omega_2$, $\vartheta_1=\vartheta_2$, and $A_1=A_2$.

The multilayer structure consists of N plane layers (Fig. 1). Each layer is assumed to be homogeneous, and is characterized by a layer thickness d_m, complex refractive indices n_{jm}, dielectric functions $\epsilon_{jm}=n_{jm}^2$, and a tensor of quadratic

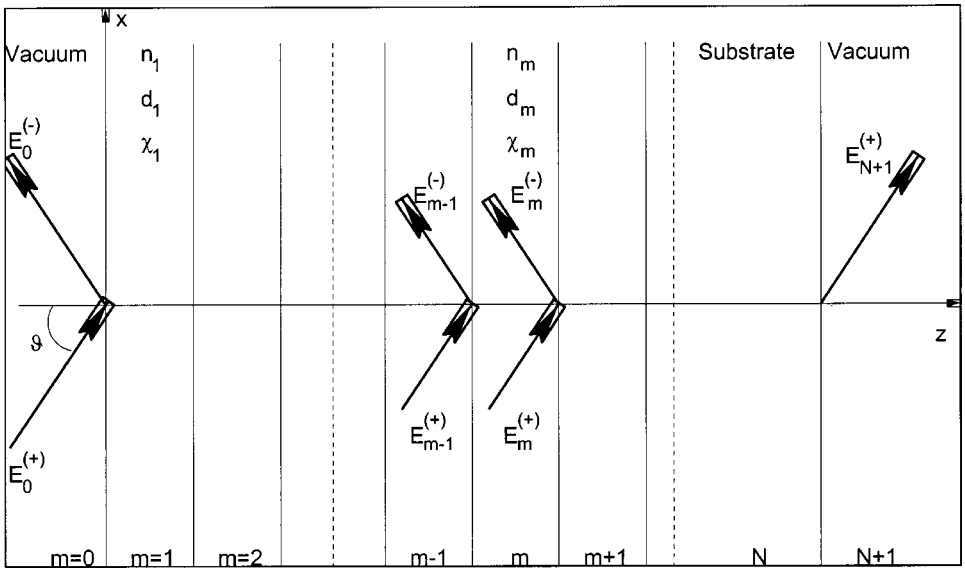

FIG. 1. Schematic of a one-dimensional multilayer nonlinear structure. n_m, d_m, and χ_m are the refractive index, the thickness, and the quadratic susceptibility of mth layer, correspondingly; N is the total number of layers; ϑ is the angle of incidence; and $E_m^{(+)}$ and $E_m^{(-)}$ are the field amplitudes of the transmitted and reflected waves in the mth layer.

susceptibility, $\hat{\chi}_m$, where the frequency index $j=1,2$, and 3; m is the layer number. The upper ($m=0$) and lower ($m=N+1$) half-infinite layers are vacuums, thus $n_{j0}=1$ and $n_{j,N+1}=1$. The Nth layer is the structure substrate.

To calculate the intensity of SF signals in areas of registration $z<0$ and $z>D$, where D is the MS thickness, one needs to solve the wave equation

$$\mathrm{rot}\,\mathrm{rot}\boldsymbol{E}(\boldsymbol{r},t)+\frac{1}{c^2}\frac{\partial^2\boldsymbol{D}(\boldsymbol{r},t)}{\partial t^2}=-\frac{4\pi}{c^2}\frac{\partial^2\boldsymbol{P}_{NL}(\boldsymbol{r},t)}{\partial t^2}, \quad (2)$$

where $\boldsymbol{D}(\boldsymbol{r},t)=\epsilon(z)\boldsymbol{E}(\boldsymbol{r},t)$ and $\boldsymbol{P}_{NL}(\boldsymbol{r},t)=\hat{\chi}:\boldsymbol{E}(\boldsymbol{r},t)\boldsymbol{E}(\boldsymbol{r},t)$ is the nonlinear polarization. To simplify the calculation we shall solve the stationary problem, neglecting the interaction of waves at different frequencies. This is permissible if the duration of the laser pulses is much larger than the propagation time of light through the sample, and if the SF wave intensity is weak compared with the intensities of the incident fundamental waves. Under this assumption, the solution of Eq. (2) within a homogeneous layer is simply a superposition of plane waves, and at the layer interface one can use boundary conditions for tangential components of the electric and magnetic fields. The nonlinear problem of SF generation is solved in the approximation of the given field of fundamental waves.

A. Linear problem

Let us obtain the extended Parratt recursion formula [22] to calculate the amplitudes of s- and p-polarized fundamental fields at the frequencies $\omega_{1,2}$ in arbitrary layer of the MS. In the case when $\boldsymbol{P}_{NL}=0$, the field $\boldsymbol{E}_{jm}(x,z)$ in the mth layer is a superposition of fundamental solutions of homogeneous Eq. (2):

$$\boldsymbol{E}_{jm}(z)=\boldsymbol{e}_j^{(+)}E_{jm}^{(+)}\exp(is_{jm}z)+\boldsymbol{e}_j^{(-)}E_{jm}^{(-)}\exp(-is_{jm}z). \quad (3)$$

Here $E_{jm}^{(+)}$ and $E_{jm}^{(-)}$ are the amplitudes of the forward and backward waves, the modulus of the wave vectors is given by $k_{jm}=k_jn_{jm}$, and the x and z components of the wave vectors are given by $(k_{jm})_x=k_{jx}=k_j\sin\vartheta_j$ and $(k_{jm})_z=\pm s_{jm}$, respectively, where

$$s_{jm}\equiv k_j[n_{jm}^2-\sin^2\vartheta_j]^{1/2}. \quad (4)$$

In expression (3) the common factor $\exp(ik_{jx}x-i\omega_jt)$ is omitted. Thus the linear problem is reduced to finding of the forward and backward wave amplitudes using the continuity of tangential components of the electric and magnetic fields.

For a plane wave $\boldsymbol{E}(\boldsymbol{r})=\boldsymbol{E}\exp(i\boldsymbol{q}\cdot\boldsymbol{r}-i\omega t)$ the electric and magnetic fields are connected by the expression $k\boldsymbol{H}=[\boldsymbol{q}\boldsymbol{E}]$, where $k=\omega/c$ and $q=[q_x^2+q_z^2]^{1/2}$. Note that the modulus is given by $q=kn$ for the homogeneous solution only. In the case of s polarization, the electric field is normal to the incident plane (x,z), i.e., $E_x=E_z=0$, and the magnetic field is in the plane ($H_y=0$). Due to the projection $q_y=0$, the tangential components of the fields are given by

$$E_y^{(\pm)}=E^{(\pm)}, \quad H_x^{(\pm)}=-(q_z/k)E^{(\pm)}. \quad (5)$$

For the homogeneous solution $q_z=\pm s$, where $s=k[n^2-\sin^2\vartheta]^{1/2}$. For the inhomogeneous solution, the vector $\boldsymbol{q}$ in the medium is determined by the sum of wave vectors at the fundamental frequencies. That is why the value q_z at the SF is a more complicated function of the values k_x and s at the frequencies $\omega_{1,2}$ [see Eq. (21) below].

In the case of p polarization, the field $\boldsymbol{E}$ is in the plane of incident; thus $E_y=0$ and $H_x=H_z=0$. Taking into account that $\boldsymbol{q}\cdot\boldsymbol{E}=0$ and $kH_y=q_zE_x-q_xE_z$, one obtains the following expressions for tangential components of the fields:

$$E_x^{(\pm)}=\pm(q_z/q)E^{(\pm)}, \quad H_y^{(\pm)}=\pm(q/k)E^{(\pm)}. \quad (6)$$

For the free wave (homogeneous solution), $q=kn$ and $q_z=\pm s$; therefore, formulas (6) are simplified to

$$E_x^{(\pm)}=(s/kn)E^{(\pm)}, \quad H_y^{(\pm)}=\pm nE^{(\pm)}. \quad (7)$$

From the conditions of continuity of tangential components of the electric and magnetic fields [Eqs. (5) and (7)] at the boundary between mth and $(m+1)$th layers, we obtain equations for the field amplitudes:

$$a_{jm}(E_{jm}^{(+)}g_{jm}+E_{jm}^{(-)}\overline{g}_{jm})=a_{j,m+1}(E_{j,m+1}^{(+)}+E_{j,m+1}^{(-)}), \tag{8a}$$

$$b_{jm}(E_{jm}^{(+)}g_{jm}-E_{jm}^{(-)}\overline{g}_{jm})=b_{j,m+1}(E_{j,m+1}^{(+)}-E_{j,m+1}^{(-)}), \tag{8b}$$

where

$$g_{jm}=\exp(is_{jm}d_m), \quad \overline{g}_{jm}\equiv g_{jm}^{-1}=\exp(-is_{jm}d_m), \tag{9}$$

$a_{jm}=1$, $b_{jm}=s_{jm}$ and $a_{jm}=s_{jm}/n_{jm}$, $b_{jm}=n_{jm}$ for s- and p-polarized waves, respectively.

Expressions (8) are the main equations that allow us to find the field amplitudes $E_{jm}^{(\pm)}$ within all layers, as well as to calculate the reflective and transmission indexes for the MS. The set of Eq. (8) is solved with the boundary conditions $E_{j0}^{(+)}=A_j$ and $E_{j,N+1}^{(-)}=0$, where $j=1$ and 2. The last condition means that the backward input field is absent at the lower boundary.

Formally, the two equations (8) for each boundary have four unknown field amplitudes. To strike off these amplitudes, the homogeneity of the equations can be used. Dividing the first equation in Eq. (8) by the second one, we obtain the Parratt recursion formula [22] that connects the reflective index $R_{jm}=E_{jm}^{(-)}/E_{jm}^{(+)}$ of the mth layer with the reflective index $R_{j,m+1}$ for the layer with number $m+1$,

$$R_{jm}=\frac{r_{jm,m+1}+R_{j,m+1}}{1+r_{jm,m+1}R_{j,m+1}}g_{jm}^2, \tag{10}$$

where

$$r_{jm,n}=p\frac{s_{jm}-s_{jn}\sigma_{jm,n}^2}{s_{jm}+s_{jn}\sigma_{jm,n}^2}, \tag{11}$$

$p=1$, $\sigma_{jm,n}=1$ and $p=-1$, $\sigma_{jm,n}=n_{jm}/n_{jn}$ for s- and p-polarized waves, respectively. Here $r_{jm,n}$ is the reflective index (Fresnel formula) of radiation at the frequency ω_j at the boundary between two half-infinite media with refractive indexes n_{jm} and n_{jn}.

The recursion problem (10) is solved with the boundary conditions $g_{j0}=1$ and $R_{j,N+1}=0$, beginning from the lower layer with number $m=N+1$. The total amplitude reflective index of the MS is R_{j0}.

From Eq. (8) we obtain a recursion formula to calculate the field amplitudes $E_{jm}^{(\pm)}$ in the arbitrary layer of the MS:

$$E_{j,m+1}^{(+)}=\sigma_{jm,m+1}\frac{g_{jm}+pR_{jm}\overline{g}_{jm}}{1+pR_{j,m+1}}E_{jm}^{(+)}. \tag{12}$$

After the finding of all reflective index R_{jm} (10), Eq. (12) is solved beginning from the upper layer with the boundary condition $E_{j0}^{(+)}=A_j$. The amplitudes of backward waves are found from the formula $E_{jm}^{(-)}=R_{jm}E_{jm}^{(+)}$.

So Eqs. (10)–(12) allow us to solve completely the problem of the fundamental-field distribution within the MS , as well as to find the values of reflective $R_j=R_{j0}=E_{j0}^{(-)}/A_j$ and transmission $T_j=E_{j,N+1}^{(+)}/A_j$ indexes.

B. Nonlinear problem of SF generation

Let us consider the problem of SF generation in a given field, which is the superposition of two fields at fundamental frequencies. According to expression (3), the fields at frequencies $\omega_{1,2}$ within the mth layer are fixed by

$$E_{jm}(x,z)=[E_{jm}^{(+)}\exp(is_{jm}z)+E_{jm}^{(-)}\exp(-is_{jm}z)]\times\exp(ik_{jx}x-i\omega_j t), \tag{13}$$

where $k_{jx}=k_j\sin\vartheta_j$ $(j=1,2)$, and the z coordinate is counted from the upper boundary of the mth layer. The field amplitudes $E_{jm}^{(\pm)}$ in Eq. (13) are known as a solution of the homogeneous linear problem [Eq. (8)] studied above.

Substitute Eq. (13) into the nonlinear polarization on the right-hand part of Eq. (2); then the solution of the equation for a SF field in a layer is the sum $E_{3m}^{s}+E_{3m}$ of inhomogeneous (index s) and homogeneous solutions. It follows from the Eq. (2) that an inhomogeneous solution at the SF $\omega_3=\omega_1+\omega_2$ is given by

$$E_{3m}^{s}(x,z)=[E_{3m}^{s(+)}\exp(is_{12m}z)+E_{3m}^{s(-)}\times\exp(-is_{12m}z)]\exp(ik_{12x}x-i\omega_3 t), \tag{14}$$

where $s_{12m}=s_{1m}+s_{2m}$ and $k_{12x}=k_{1x}+k_{2x}$; i.e., the projections of the wave vectors of plane waves [Eq. (14)] equal to the sum of the corresponding projections of wave vectors at the fundamental frequencies. The amplitudes of these waves are proportional to the products of field amplitudes at the fundamental frequencies

$$E_{3m}^{s(\pm)}=\frac{4\pi\chi_m}{\Delta_m}E_{1m}^{(\pm)}E_{2m}^{(\pm)}, \tag{15}$$

where

$$\Delta_m=(s_{12m}^2+k_{12x}^2-k_3^2n_{3m}^2)/k_3^2, \quad \chi_m=\boldsymbol{e}_3\hat{\chi}_m\boldsymbol{e}_1\boldsymbol{e}_2. \tag{16}$$

The value Δ_m is fixed by the dispersion of refractive indexes n_{jm} $(j=1,2,3)$ and by the spatial orientation of wave vectors of the incident radiation at fundamental frequencies, i.e., by the angles of incidence $\vartheta_{1,2}$.

Due to the condition of continuity of the tangential components of the wave vectors at layer boundaries, the x projections of the wave vectors of free waves (homogeneous solution) and stimulated wave [Eq. (14)] (inhomogeneous solution) are equal: $k_{3x}=k_{1x}+k_{2x}$. Since the modulus of the wave vector at the SF in vacuum is $k_3=\omega_3/c=k_1+k_2$, the angle of output of the SF radiation in vacuum is fixed by the equation

$$k_3\sin\vartheta_3=k_1\sin\vartheta_1+k_2\sin\vartheta_2. \tag{17}$$

It follows from this equation that in the case of collinear rays ($\vartheta_1=\vartheta_2$) at fundamental frequencies, the angle $\vartheta_3=\vartheta_1$, and formula (16) for SH ($\omega_1=\omega_2$) is simplified to

$$\Delta_m=n_{1m}^2-n_{3m}^2.$$

We seek the solution of the homogeneous equation (2) ($\boldsymbol{P}_{NL}=0$) for radiation at frequency ω_3 within the mth layer in the form

$$E_{3m}(x,z)=[E_{3m}^{(+)}\exp(is_{3m}z)+E_{3m}^{(-)}\exp(-is_{3m}z)]\times\exp(ik_{3x}x-i\omega_3 t), \tag{18}$$

where s_{3m} is fixed by the expression

$$s_{3m}=k_3(n_{3m}^2-\sin^2\vartheta_3)^{1/2}. \tag{19}$$

Using Eq. (19), the expression for the parameter of phase matching Δ_m [Eq. (16)] takes the form

$$\Delta_m=[(s_{1m}+s_{2m})^2-s_{3m}^2]/k_3^2.$$

The nonlinear problem for SF generation is formulated as follows: taking into account the boundary conditions for both the forward SF wave ($E_{3,0}^{(+)}=0$ if $z<0$) and the backward wave ($E_{3,N+1}^{(-)}=0$ if $z>D$), one needs to find the amplitudes of homogeneous solutions $E_{3,0}^{(-)}$ and $E_{3,N+1}^{(+)}$ in the areas of registration in vacuum.

The conditions of continuity for tangential components of electric and magnetic fields at each $N+1$ layer boundaries lead to the necessity to of solving the set of $2(N+1)$ inhomogeneous linear equations for the SF field amplitudes $E_{3m}^{(\pm)}$. Taking into account expressions (5) and (6), these equations at the boundary between mth and $(m+1)$th layers take the following forms (we omit below the SF index $j=3$ for $E_{3m}^{(\pm)}$, g_{3m}, s_{3m}, and n_{3m}):

$$a_mF_m^{(1)}+\alpha_mS_m^{(1)}=a_{m+1}F_{m+1}^{(3)}+\alpha_{m+1}S_{m+1}^{(3)}, \tag{20a}$$

$$b_mF_m^{(2)}+\beta_mS_m^{(2)}=b_{m+1}F_{m+1}^{(4)}+\beta_{m+1}S_{m+1}^{(4)}, \tag{20b}$$

where

$$F_m^{(1,2)}=E_m^{(+)}g_m\pm E_m^{(-)}\overline{g}_m,\quad F_m^{(3,4)}=E_m^{(+)}\pm E_m^{(-)},$$

$$S_m^{(1,2)}=E_m^{s(+)}f_m\pm E_m^{s(-)}\overline{f}_m,\quad S_m^{(3,4)}=E_m^{s(+)}\pm E_m^{s(-)}.$$

Here $a_m=a_{3m}$, $b_m=b_{3m}$, and $g_m=\exp(is_md_m)$, [Eq. (9)]; $f_m=g_{1m}g_{2m}$; $\alpha_m=1$, and $\beta_m=s_{1m}+s_{2m}$; and $\alpha_m=(s_{1m}+s_{2m})/n_m^{(s)}$ and $\beta_m=n_m^{(s)}$ for s- and p-polarized radiation, respectively. The ''refractive index'' for the stimulated wave is $n_m^{(s)}=k_{3m}^{(s)}/k_3$, where the modulus of the wave vector is

$$k_{3m}^{(s)}=[(s_{1m}+s_{2m})^2+k_3^2\sin^2\vartheta_3]^{1/2}. \tag{21}$$

In the special case of collinear SH generation, the formula simplifies to $n_m^{(s)}=n_{1m}$.

To solve Eqs. (20) we shall use the following well-known theorem. The root of a set of N linear inhomogeneous equations $\Sigma_j a_{ij}x_j=b_i$ can be taken in the form of a sum of N items $x_j=\Sigma_k x_{jk}$. Each item is a solution of the set of equations $\Sigma_j a_{ij}x_{jk}=\delta_{ik}b_i$, in which one equation is inhomogeneous while the other equations are homogeneous (δ_{ik} is the Kroneker symbol). Therefore, at the beginning we need to find the field amplitudes at the SF in vacuum $E_{3,0}^{(-)}(m)$ and $E_{3,N+1}^{(+)}(m)$ under the condition that nonlinear susceptibility takes place only in one layer with number m. In this case the SF wave propagates above and below the mth layer as a free wave obeying Eqs. (8), where $j=3$. The final result is obtained by a summation over all nonlinear mth layers of the values $E_{3,0}^{(-)}(m)$ and $E_{3,N+1}^{(+)}(m)$. The correctness of this procedure also follows from the principle of superposition for SF waves.

Let us consider three neighboring layers with numbers $m-1$, m, and $m+1$; the mth layer has $\chi_m\neq 0$. Strike off the amplitudes $E_m^{(\pm)}$ from Eqs. (20) that are written for boundaries between the $(m-1)/m$th and $m/(m+1)$th layers. As a result, we obtain the following connection between amplitudes $E_{m-1}^{(\pm)}$ and $E_{m+1}^{(\pm)}$ in upper and lower linear layers:

$$H_{11}E_{m+1}^{(+)}-H_{12}E_{m-1}^{(-)}=Q_m, \tag{22a}$$

$$H_{21}E_{m+1}^{(+)}-H_{22}E_{m-1}^{(-)}=P_m, \tag{22b}$$

where

$$H_{11}(m)=\overline{g}_m(1+r_{m,m+1}R_{m+1})/t_{m,m+1},$$

$$H_{12}(m)=(r_{m,m-1}\overline{g}_{m-1}+T_{m-1}g_{m-1})/t_{m,m-1},$$

$$H_{21}(m)=g_m(r_{m,m+1}+R_{m+1})/t_{m,m+1}, \tag{23}$$

$$H_{22}(m)=(\overline{g}_{m-1}+r_{m,m-1}T_{m-1}g_{m-1})/t_{m,m-1}.$$

The right hand parts of Eqs. (22) have the forms

$$Q_m=\tau_m^{(+)}(f_m\overline{g}_m-1)E_m^{s(+)}+\tau_m^{(-)}(\overline{f}_m\overline{g}_m-1)E_m^{s(-)},$$

$$P_m=\tau_m^{(-)}(f_mg_m-1)E_m^{s(+)}+\tau_m^{(+)}(\overline{f}_mg_m-1)E_m^{s(-)}, \tag{24}$$

where

$$t_{mn}=2s_m\sigma_{mn}/(s_m+s_n\sigma_{mn}^2),$$

$$\tau_m^{(+)}=(s_m+s_{12m}\nu_m^2)/2s_m\nu_m,$$

$$\tau_m^{(-)}=p(s_m-s_{12m}\nu_m^2)/2s_m\nu_m.$$

Here $T_m=1/R_m$, and t_{mn} is the Fresnel transmission index for the boundary between two media with refractive indexes n_m and n_n; the reflective indexes r_{mn} are fixed by Eq. (11) where $j=3$; $p=1$, $\nu_m=1$ and $p=-1$, $\nu_m=n_m/n_m^{(s)}$ for s- and p-polarized SF radiation, respectively.

Let us take advantage of recursion formulas that connect the field amplitude $E_m^{(+)}$ in the mth layer with the amplitude $E_{m+1}^{(+)}$ in the lower layer with a number $m+1$, as well as the amplitude $E_m^{(-)}$ with the amplitude $E_{m-1}^{(-)}$ in the upper layer with a number $m-1$. From expressions (12) and (10) we obtain general recurrence relations for the nonlinear problem:

$$E_m^{(+)}=A_m E_{m+1}^{(+)}, \quad E_m^{(-)}=B_m E_{m-1}^{(-)}, \tag{25}$$

where

$$A_m=\frac{1+pR_{m+1}}{g_m+pR_m\overline{g}_m}\sigma_{m+1,m},$$
$$B_m=\frac{\overline{g}_{m-1}+pT_{m-1}g_{m-1}}{1+pT_m}\sigma_{m-1,m}. \tag{26}$$

The coefficients R_m for A_m are found by solving problem (10) (where $j=3$) with the boundary condition $R_{N+1}=0$, beginning from the lower layer with the number $m=N+1$. The values T_m for B_m are obtained by using the following recursion formula:

$$T_m=\frac{r_{m,m-1}+T_{m-1}g_{m-1}^2}{1+r_{m,m-1}T_{m-1}g_{m-1}^2}. \tag{27}$$

This formula follows from Eq. (10), where $j=3$, and is solved with the boundary condition $T_0=0$ beginning from the upper layer.

Successively using formulas (25), it is not hard to obtain the following expressions for the SF field amplitudes that come into Eq. (22):

$$E_{m+1}^{(+)}=A(m)E_{N+1}^{(+)}, \quad E_{m-1}^{(-)}=B(m)E_0^{(-)}, \tag{28}$$

where $A(m)$ and $B(m)$ are products of coefficients (26):

$$A(m)=A_{m+1}A_{m+2},\ldots,A_{N-1}A_N,$$
$$B(m)=B_{m-1}B_{m-2},\ldots,B_2B_1. \tag{29}$$

Substituting Eq. (28) into Eq. (22) and solving the equations, we obtain final expressions for the amplitudes of SF fields in the areas of registration due to one nonlinear mth layer:

$$E_0^{(-)}(m)=(H_{21}Q_m-H_{11}P_m)/D_mB(m),$$
$$E_{N+1}^{(+)}(m)=(H_{22}Q_m-H_{12}P_m)/D_mA(m), \tag{30}$$

where $D_m=H_{11}H_{22}-H_{21}H_{12}$ is the determinant of set (22); the values H_{ij} are fixed by Eq. (23), and $A(m)$ and $B(m)$ by Eq. (29).

The total amplitudes of reflected and transmitted waves generated by the MS are calculated as a sum over the nonlinear layers of the partial amplitudes (30). The intensities of reflected and transmitted SF signals are fixed by the expressions

$$I_{SF}^{(-)}=|E_{SF}^{(-)}|^2=\left|\sum_{m=1}^{N}E_0^{(-)}(m)\right|^2,$$
$$I_{SF}^{(+)}=|E_{SF}^{(+)}|^2=\left|\sum_{m=1}^{N}E_{N+1}^{(+)}(m)\right|^2. \tag{31}$$

III. SECOND HARMONIC AND SUM-FREQUENCY GENERATION UNDER QUASIPHASE MATCHING CONDITIONS. ROLE OF THE NONPHASE MATCHING ENHANCEMENT OF NONLINEAR OPTICAL SIGNALS

The recurrence relation method described in this paper allows us to take into account correctly the contributions of all mechanisms of enhancement of the nonlinear optical response (phase matching, quasiphase matching, and nonphase matching) in SH and SF generation processes for transmitted and reflected fields, as well for different polarizations of incoming and generated waves. For a multilayer structure, described in Sec. IV of this paper, that consists of ''linear'' (SrF_2) and ''nonlinear'' (ZnS) layers, we discuss the optimization conditions for SF and SH generation in the reflection geometry.

In Fig. 2(a) we show the angular dependencies of the reflection coefficient $R(\vartheta)$ (dashed curve) and the angular tuning curve for the distribution of the field energy at the fundamental frequency in ''nonlinear'' layers $I_1(\vartheta)=\Sigma_m|E_{1m}^{(-)}|^2$ (solid curve), calculated according to Eqs. (10) and (12). The maxima of the energy of the field are localized near the edges of the Bragg forbidden zone. However, if we assume that the value of the refraction index of the nonlinear layer at the SH frequency as $n_{1,SH}=2.75$, the maximum of the SH intensity reflected from the structure $I_{SH}^{(-)}$ [Eq. (31)] is situated outside of the area of the maximal energy concentration at the fundamental frequency [Fig. 2(b)]. The position of the SH maximum is determined by the sixth order QPM. Let us show this, estimating the phase mismatching parameter Δ for a z projection of the effective wave vectors s_j^{ef} of the fields in the structure:

$$\Delta(\vartheta)=[2s_1^{ef}(\vartheta)+s_3^{ef}(\vartheta)-Gl]d,$$

where $G=2\pi/d$ is the absolute value of the reciprocal lattice vector, $d=d_1+d_2$ is the period of the structure, and l is the order of QPM. The value s_j^{ef} is determined by Eq. (4), where, instead of the refraction indexes of separate layers of the multilayer structure n_{jm}, we used the effective (common for whole structure) refractive index $n_j^{ef}(\vartheta)$, calculated from the dispersion equation [23], modified for an arbitrary angle of incidence ϑ,

$$\cos(s_j^{ef}d)=\cos(s_{j1}d_1)\cos(s_{j2}d_2)$$
$$-\frac{1}{2}\left(\frac{\sigma_{j12}s_{j1}}{s_{j2}}+\frac{s_{j2}}{\sigma_{j12}s_{j1}}\right)\sin(s_{j1}d_1)\sin(s_{j2}d_2),$$

where $s_{j1,2}$ are z projections of the field wave vectors at frequencies ω_j in even and odd layers with refractive indexes

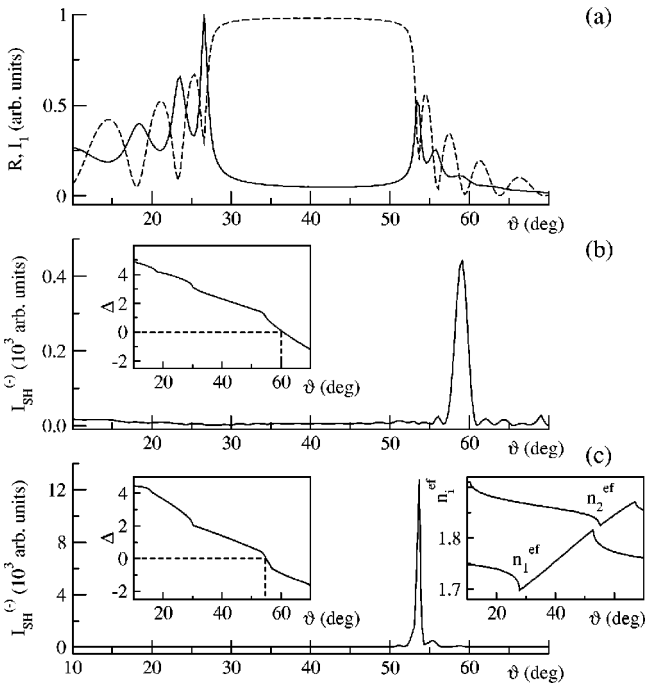

FIG. 2. (a) Linear reflection coefficient R (dashed line), and the sum of the fundamental field energy inside the nonlinear layers of the structure I_1 (solid line) versus the angle of incidence of the radiation with the wavelength $\lambda_1=720$ nm. The refractive index of the nonlinear layers is $n_1=2.327$, that of the linear layers is $n_2=1.435$, and the number of periods of the structure is $N=20$. (b) and (c) Intensities of the reflected second-harmonic signal $I_{SH}^{(-)}$ for the following values of the refractive indexes of the layers at the second harmonic frequency: (b) $n_{1,SH}=2.75$, $n_{2,SH}=1.45$; (c) $n_{1,SH}=2.55$, and $n_{2,SH}=1.45$. In the insets we show the phase mismatching parameter Δ and the effective refractive indexes at the fundamental frequency n_1^{ef} and at the second harmonic frequencies n_2^{ef} vs the angle of incidence of the radiation.

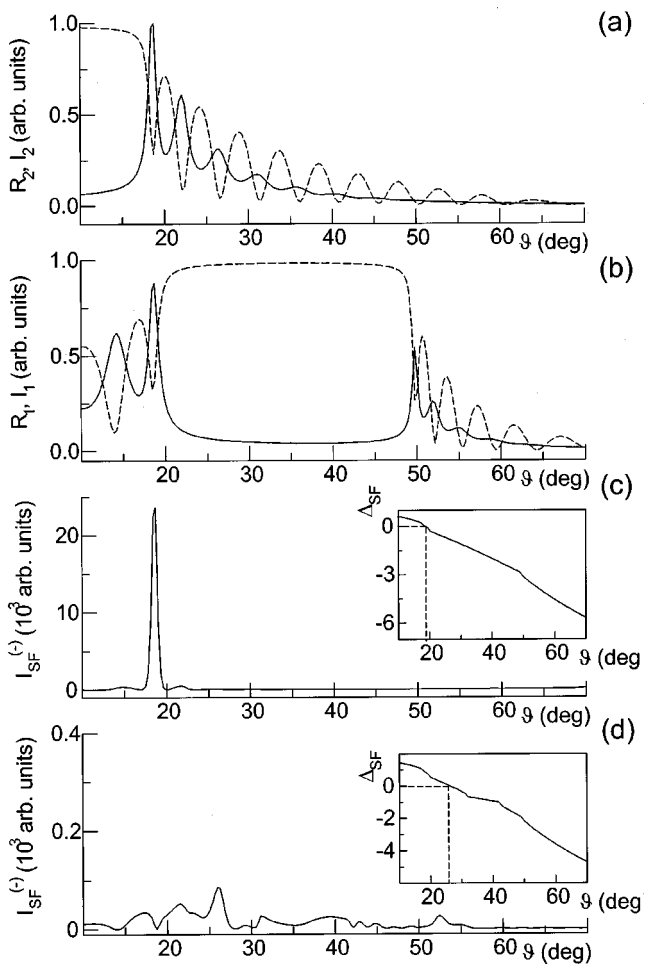

FIG. 3. (a) and (b) Linear reflection coefficient $R_{1,2}$ (dashed line) and the density of the electromagnetic field inside the nonlinear layers of the multilayer structure $I_{1,2}$ (solid line) vs the angle of incidence of the radiation with wavelengths $\lambda_2=813$ nm (a) and $\lambda_1=736$ nm (b). Refractive indexes of the nonlinear layers $n_1(\lambda_2)=2.311$ and $n_1(\lambda_1)=2.33$; for linear layers, $n_2(\lambda_2)=1.434$, and $n_2(\lambda_1)=1.435$; the number of the periods $N=20$. (c) and (d) Intensity of the reflected SF signal $I_{SF}^{(-)}$ for the following values of the refractive indexes of the layers at the SF: (c) $n_{1,SF}=2.3$ and $n_{2,SF}=1.445$ and (d) $n_{1,SF}=2.5$ and $n_{2,SF}=1.445$. In the insets we show the phase mismatching parameters Δ_{SF} vs the angle of incidence of the radiation.

n_{j1} and n_{j2}, consequently $(j=1,2,3)$; $d_{1,2}$ are the thicknesses of these layers; $s_j^{ef}=k_j[(n_j^{ef})^2-\sin^2\vartheta]^{1/2}$; $\sigma_{j12}=1$ and $\sigma_{j12}=n_{j1}/n_{j2}$ for s and p polarizations of the fields, consequently. In the inset of Fig. 2(b) the angular dependence of the $\Delta(\vartheta)$ function for the sixth order QPM ($l=6$) is presented. The value of the angle of incidence when the QPM condition are fulfilled $\Delta=0$ [12] is the same as the angular position of the maximum of the SH intensity.

A considerable increase of the SH generation efficiency may be achieved in the case of a shift of the QPM condition into the area of angles closer to the edge of the Bragg forbidden zone. Near the PBG edge there is a maximal localization of the field energy at a fundamental frequency, and due to this a nonphase matching mechanism of enhancement takes place. Actually, when we decrease the value $n_{1,SH}$, we shift of the QPM maximum into a smaller angular area, and we observe an increase of 30 times the SH intensity at the right edge of the PBG [Fig. 2(c); $n_{1,SH}(\mathrm{ZnS})=2.55$]. We also note, and demonstrate in the right inset to the Fig. 2(c), that at the right side of the PBG the value of $n_2^{ef}-n_1^{ef}$ becomes minimal. Due to this the dispersive phase matching conditions are closer to being fulfilled. However, the contribution of the QPM mechanism to the efficiency of the SH generation process is much greater than the contribution of the dispersive one. This is due to the fact that the intensity of the reflected SH is in six times more than the intensity of the transmitted signal.

Let us consider the enhancement of SF generation near the photonic band gap edges under QPM condition. The incident angles of two laser pulses at frequencies ω_1 and ω_2 are assumed to be identical. The frequencies are chosen near the opposite edges of a given Bragg band gap. In this case, the edges of two linear reflection curves $R_1(\vartheta)$ and $R_2(\vartheta)$ will be located in the same angular range [Figs. 3(a) and 3(b)]. This leads to a simultaneous increase of the energies of both fields $I_1(\vartheta)=\Sigma_m|E_{1m}^{(-)}|^2$ and $I_2(\vartheta)=\Sigma_m|E_{2m}^{(-)}|^2$ at the

fundamental frequencies ω_1 and ω_2 inside the structure. That is, the optimum for nonphase matching enhancement is realized. In Fig. 3(c) and 3(d) the angular dependencies of the intensity of the signals at the sum frequency $\omega_3=\omega_1+\omega_2$, calculated according to Eqs. (30) and (31), are shown. Figure 3(c) demonstrates the situation when both conditions for QPM, $\Delta_{SF}=0$ and nonphase matching enhancement, are fulfilled completely, where

$$\Delta_{SF}(\vartheta)=[s_1^{ef}(\vartheta)+s_2^{ef}(\vartheta)+s_3^{ef}(\vartheta)-Gl]d,$$

and $l=6$. In contrast, in Fig. 3(d) the QPM condition is achieved at a larger angle, and, as a result, the SF intensity decreases to more then two orders of magnitude.

We would like to note here that there is an additional way to achieve the QPM for the SF generation in the case of noncollinear wave interaction, when the QPM parameter Δ_{SF} has the form

$$\Delta_{SF}(\vartheta_1,\vartheta_2)=[s_1^{ef}(\vartheta_1)+s_2^{ef}(\vartheta_2)+s_3^{ef}(\vartheta_3)-Gl]d,$$

where ϑ_1 and ϑ_2 are the angles of incidence of two fundamental waves; $s_j^{ef}(\vartheta_j)$ are fixed by expressions (4) and (19) for the effective refractive indexes $n_j^{ef}(\vartheta_j)$; and the angle ϑ_3 is calculated from Eq. (17). For the wide range of angles ϑ_1 we may find the angles ϑ_2 to satisfy the QPM condition $\Delta_{SF}=0$ for the chosen pair of wavelengths of the fundamental beams.

IV. EXPERIMENTAL SETUP AND SAMPLE PREPARATION

In our experiments we considered SF and SH generation from one-dimensional PBG material prepared in the form of a multilayer structure described in Ref. [17]. The structure is composed of 15 alternate layers deposited on a glass substrate—eight layers have high (ZnS, $n_1=2.3$) refractive indexes and seven have low (SrF_2, $n_2=1.43$) refractive indexes. Then, for the chosen wavelength $\lambda_0=785$ nm, the layers have a thickness $d_i=3\lambda_0/(4n_i)$ and the total structure thickness is $L=4.9\mu$m. This periodic structure forms the PBG in a wavelength range of 780–810 nm at normal incidence of the light beam.

The sample was studied using a setup (Fig. 4) based on laser sources that are produced by Coherent Inc. [24]. The output pulses of a femtosecond mode-locked Ti:sapphire laser Mira 900 are regeneratively amplified with RegA 9000 up to $W_p=4$ μJ/pulse at a 200-kHz repetition rate. Part of the RegA laser radiation is seeded into optical parametric amplifier OPA 9400 to produce tunable light, which is used as a ω_1 beam in the sum frequency process ($\omega_{SF}=\omega_1+\omega_2$). The range of the OPA tunability is 500–750 nm, the minimal pulse duration is 250 fs, and the average power is 10 mW (after a special filtration by means of a spatial spectral filter) [25]. The rest of the RegA output forms a second beam ω_2, necessary for the sum frequency signal generation. The minimal pulse duration for the ω_2 radiation is 270 fs, and the central wavelength of the pulse spectrum is in the range of 810–820 nm with a 10-mW average power. To

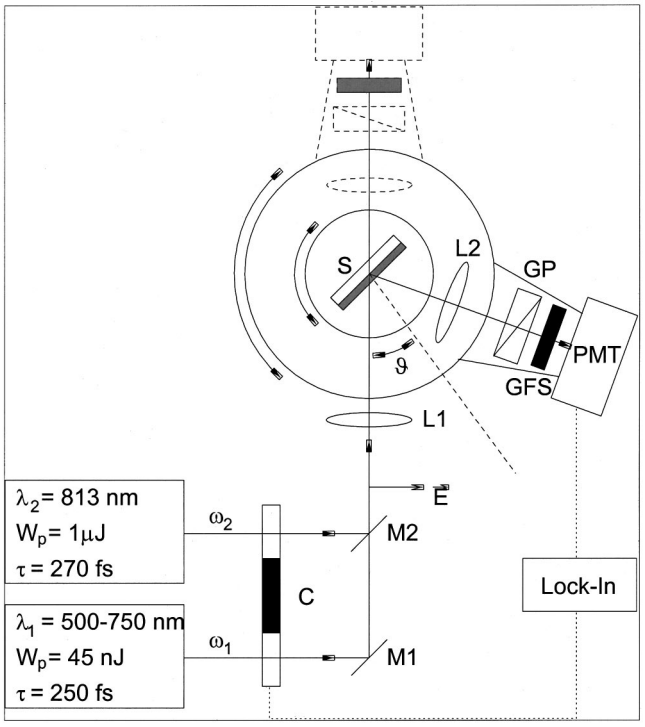

FIG. 4. Experimental setup. C is the mechanical chopper; $M1$ and $M2$ are the dichroic mirrors; $L1$ and $L2$ are the lenses; S is the sample; GFS is the set of glass filters; GP is the Glan-Taylor polarizer; PMT is the photomultiplier tube; and Lock-In is the lock-in amplifier.

overlap ω_1 and ω_2 pulses in time, a delay line is inserted into the ω_2 beam path. We used two pairs of Glan-Taylor polarizers in both beams ω_1 and ω_2 in order to vary the average power of radiation coming to the MS sample. The average power in each beam during the measurements was adjusted to 1 mW. The polarization of the ω_2 incident beam was set to be either parallel (p polarization) or perpendicular (s polarization) to the plane of incidence with a double Fresnel rhombus. The polarization of the ω_1 beam was fixed in the plane of incidence (p polarization). The beams are overlapped to be collinear, and are focused into a sample with a 76-mm lens ($L1$). The sample (S) is mounted on the rotation stage DMT 65 (OWIS) in order to vary and align incident angles.

The receiving part (Fig. 4) of the experimental setup consists of a collimating lens ($L2$), a Glan Taylor prism GP to select the p-polarized component of the sum frequency signal, and a set of glass filters (SGF) to reject scattering light coming from ω_1 and ω_2 beams. The signal registration is realized with Hamamatsu R-4220P photomultiplier tube (PMT) connected with lock-in-amplifier EEG-5110 (EG&G) for synchronous detection. The radiation in both beams was modulated by means of a chopper (C). It chops ω_1 and ω_2 beams with frequencies $f_1\sim628$ Hz and $f_2\sim383$ Hz, respectively. The frequency of the detection was chosen as $f_1+f_2=1011$ Hz. The receiving part is held on another arm of the rotation stage. In our experiments we used two schemes for the signal registration: ''in transmission'' geometry and ''in reflection'' geometry.

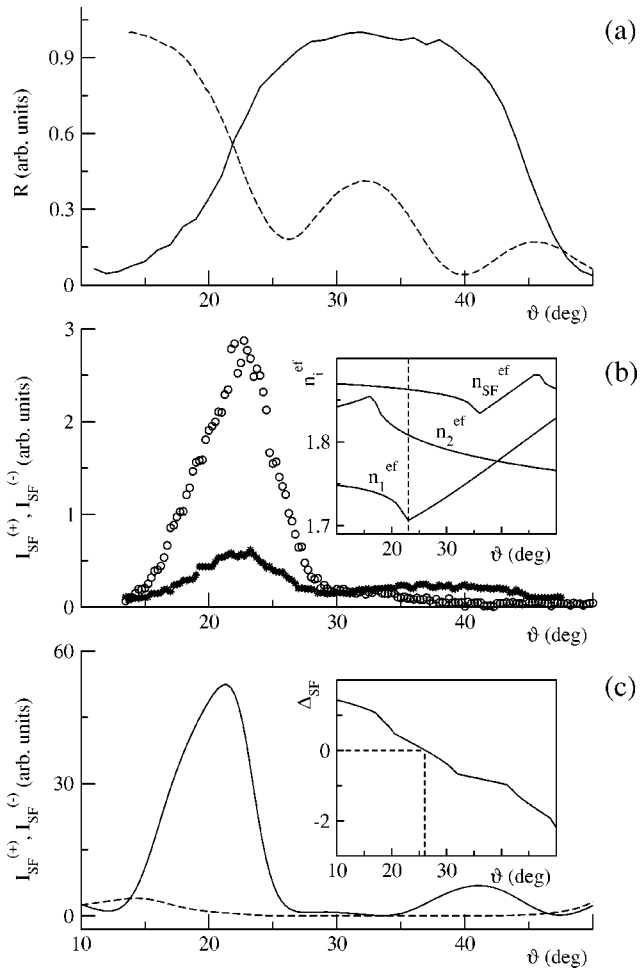

FIG. 5. (a) Experimental measurements of the linear reflection of light with wavelengths $\lambda_1=736$ nm (solid line) and $\lambda_2=813$ nm (dashed line), vs the angle of incidence on the structure. (b) Experimental measurements of the sum-frequency transmitted $I_{SF}^{(+)}$ ($\star$) and reflected $I_{SF}^{(-)}$ ($\bigcirc$) signals. (c) Calculated intensities of the transmitted $I_{SF}^{(+)}$ (dashed line) and reflected $I_{SF}^{(-)}$ (solid line) SF signals. The refractive indexes of the ZnS layers are $n_1(\lambda_2)=2.311$, $n_1(\lambda_1)=2.33$, $n_1(SF)=2.5$; these of the SrF_2 layers are $n_2(\lambda_2)=1.434$, $n_2(\lambda_1)=1.435$, and $n_2(SF)=1.442$. In the insets to (b) and (c) we show the culculated effective refractive indexes at the fundamental frequencies $n_{1,2}^{ef}$ and at the SF n_{SF}^{ef}, and the phase mismatching parameter Δ_{SF} of the sixth-order QPM for the reflected signal vs the angle of incidence of the radiation.

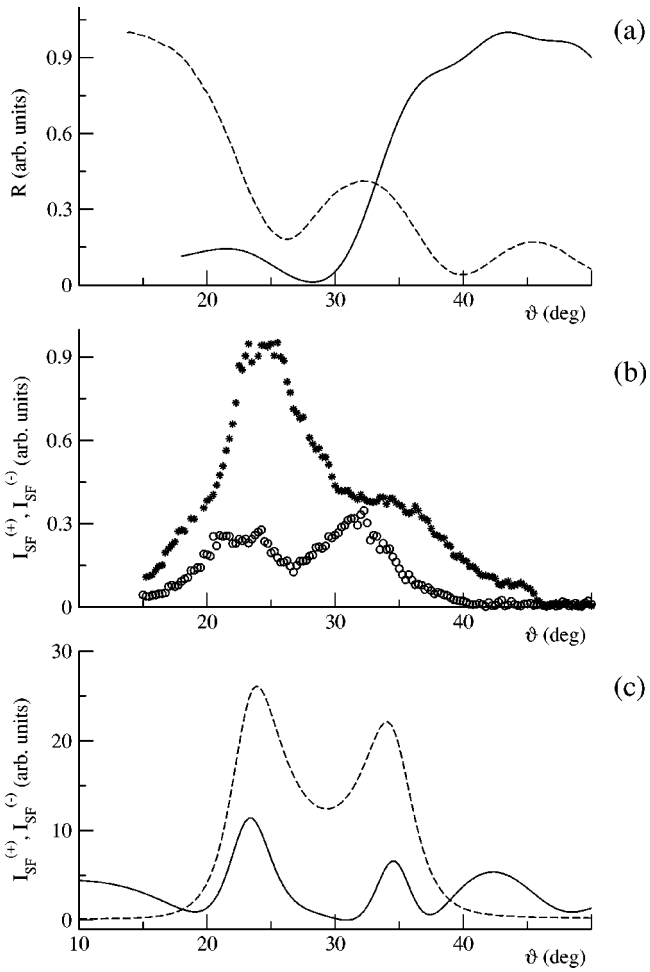

FIG. 6. (a) Experimental measurements of the linear reflection of light at wavelengths $\lambda_1=703$ nm (solid line) and $\lambda_2=813$ nm (dashed line), vs the angle of incidence on the structure. (b) Experimental measurements of the sum-frequency transmitted $I_{SF}^{(+)}$ ($\star$) and reflecteed $I_{SF}^{(-)}$ ($\bigcirc$) signals. (c) Calculated intensities of the transmitted $I_{SF}^{(+)}$ (dashed line) and reflected $I_{SF}^{(-)}$ (solid line) SF signals vs the angle of incidence of the radiation.

The wavelengths of ω_1 and ω_2 beams and ω_{SF} signal are controlled by us of a spectrograph (Chromex 500IS), with a liquid nitrogen cooled back-illuminated CCD detector (Princeton Instruments Inc.). This equipment is not depicted in the scheme.

V. EXPERIMENTAL RESULTS AND DISCUSSION

The possibility of a nonphase matching enhancement of the nonlinear optical signal concerned with field localization at a fundamental frequency was predicted in Ref. [16], and demonstrated experimentally in Refs. [17,18]. The purpose of the experiments presented in this paper was concerned with a clarification of the action of the QPM together with the nonphase matching enhancement. For this we performed two series of measurements.

We first studied the properties of both reflected and transmitted signals at SF versus the angle of incidence on the PBG structure. These measurements were performed for two sets of wavelengths of the ω_1 beam, $\lambda_1=736$ and 703 nm; the wavelength λ_2 of the ω_2 beam was fixed at $\lambda_2=813$ nm. The polarization directions of both FF beams was set to be ''*p*.''

Figures 5(a) and 5(b) and 6(a) and 6(b) show the experimental measurements of the angular behavior of the FF pulse reflection (a), as well as the transmitted and reflected SF signals (b). In Figs. 5(a) and 6(a), the solid lines represent reflection in the linear regime for the $\lambda_1=736$ and 703 nm, correspondingly; the linear reflection curve for the $\lambda_2=813$ nm is the same for both figures, and is represented by the dashed lines. All linear reflection curves are normalized at their maximum values. The intensity of the SF signal is

given in arbitrary units, and the units in Figs. 5 and 6 are the same. Thus we may compare the efficiency of transmitted ($\star$) and reflected ($\bigcirc$) SF signals for the two pairs of wavelengths.

We find that the resulting relative shift of angular positions of band edges for two chosen different wavelengths of $\lambda_1 = 736$ and 703 nm leads to dramatic changes in the intensities of the SF signal. First of all, the ratio between the intensity of the transmitted and reflected SF signals changes: the reflected SF intensity, higher with $\lambda_1 = 736$ nm, becomes lower than the transmitted one in the case of $\lambda_1 = 703$ nm. Moreover, the angular profiles of the signals change. For $\lambda_1 = 703$ nm [Fig. 6(b)] two peaks in the SF generation angular dependence, of around 24° and 32°, are observed.

These experimental results agree with the theoretical prediction [Figs. 5(c) and 6(c)]. For the first set of two wavelengths $\lambda_1 = 736$ nm and $\lambda_2 = 813$ nm, the conditions for the nonphase matching enhancement are optimal at the PBG edges around the $\vartheta = 22°$ [Fig. 5(c)]. Moreover, at the SF $\lambda_3 = 386$ nm, the QPM condition are approximately fulfilled. From the inset to Fig. 5(c) it is seen that the exact QPM is fulfilled at an angle of incidence of 26°, and the inset of Fig. 5(b) demonstrates that this is truly QPM, and not dispersive phase matching. However, the maximum of the reflected SF signal is localized at 22°. We may conclude that under experimental conditions for the wavelengths $\lambda_1 = 736$ nm and $\lambda_2 = 813$ nm the angular position of SF peak is determined by the conditions of nonphase matching enhancement, while the values of reflected and transmitted SF signals are determined both by the nonphase matching enhancement and QPM interaction. Actually, the simulation shows that in the studied PBG structure at band edges the energy of the forward-propagating FF waves in nonlinear layers always exceed the energy of the backward-propagating waves $\Sigma_m |E^{(+)}_{1,2m}|^2 > \Sigma_m |E^{(-)}_{1,2m}|^2$. Thus, if the enhancement of the SF signal is caused mainly by the nonphase matching mechanism, the intensity of the transmitted SF wave exceeds the intensity of the reflected one. The opposite correlation of intensities of transmitted and reflected SF waves [Figs. 5(b) and 5(c)] testifies that nonphase matching enhancement and QPM interaction take place simultaneously in our experiment.

Figure 6(c) shows the theoretical angular dependencies of intensities of reflected (solid curve) and transmitted (dashed curve) SF signals for the wavelength combinations $\lambda_1 = 703$ nm and $\lambda_2 = 813$ nm. We see a rather good agreement with experimental data [Fig. 6(b)]. The edges of the reflection curves do not cross in the range of 20°–40° [Fig. 6(a)], and, for this reason, the conditions for the nonphase matching enhancement are not satisfied simultaneously for both wavelength. The QPM condition is fulfilled at an angle of incidence $\vartheta = 35°$, but at these angles the density of the FF field at ω_2 is low enough, and the role of the non-phase-matching enhancement is weak. As a result, there is only a weak enhancement of the reflected SF signal. The intensity of the transmitted SF radiation is higher compared with the reflected one [Figs. 6(b) and 6(c)], and concerned with the higher energy of the forward propagating FF in nonlinear layers.

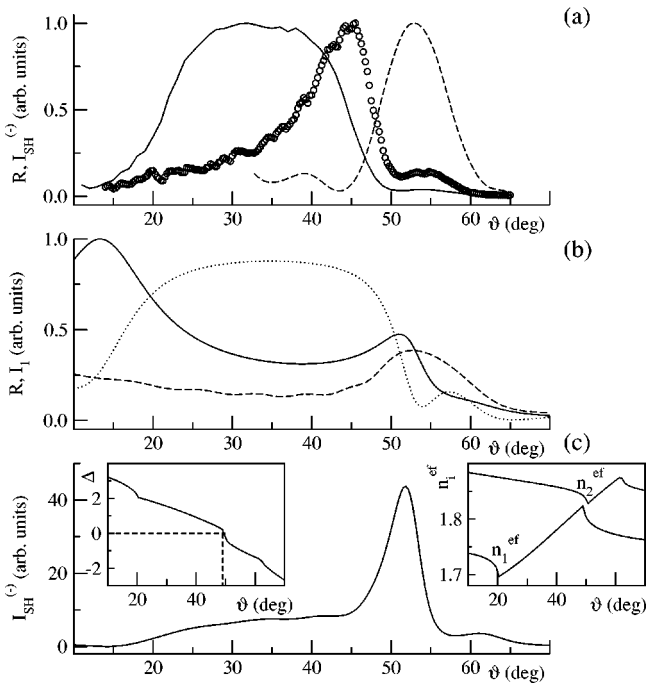

FIG. 7. (a) Experimental measurements of the linear reflection of radiation at the fundamental wavelength $\lambda_1 = 736$ nm (solid line) and at the SH wavelength $\lambda_2 = 368$ nm (dashed line), and the intensity of the reflected second-harmonic $I^{(-)}_{SH}$ signal ($\bigcirc$) vs the angle of incidence of the radiation on the sample. (b) Calculated linear reflection coefficient R at the FF (dotted line) and at SH (dashed line) frequency, as well as the density of the electromagnetic field at the FF inside the nonlinear layers of multilayer structure I_1 (solid line) vs the angle of incidence on the structure. (c) Calculated intensity of the reflected SH signal $I^{(-)}_{SH}$. The refractive indexes of the layers at the SH frequency are $n_{1,SH} = 2.55$ and $n_{2,SH} = 1.45$. In the insets we show the phase mismatching parameter Δ, as well as the effective refractive index at the FF, n_1^{ef}, and at the SH frequency, n_2^{ef}, vs the angle of incidence.

Second, we measured the efficiency of the second harmonic generation process, as a particular case of sum frequency generation, versus the angle of incidence on the PBG structure. Figure 7(a) shows the results of the SH generation measurements (open circle), where we used only one beam ω_1 with a wavelength $\lambda_1 = 736$ nm. In Fig. 7(a) the solid line corresponds to the angular dependence of the linear reflection coefficient for a beam at a fundamental wavelength, and the dashed line corresponds to the SH wavelength ($\lambda_{SH} = 368$ nm). Both curves are normalized to them maximum values. To record the linear reflection curve for the SH wavelength, we generate the second harmonic signal before the PBG sample (just before the focusing lens $L1$; see Fig. 4) using the thin LBO crystal. In linear reflection experiments incoming beams at both fundamental and SH frequencies were p polarized.

The SH intensity reaches a maximum at angles where the edges of Bragg reflected curves at both FF and SH frequency are crossed together. In this angular region the effective refractive index at the FF n_1^{ef} increases, and the effective re-

fractive index at the SH frequency n_2^{ef} decreases, which may lead to the achievement of phase matching conditions in spite of the high material dispersion of the sample. The calculations show [Fig. 7(b) and 7(c)] that in our experiment at the PBG edge the conditions of QPM and nonphase matching enhancement are fulfilled simultaneously. Moreover, the phase matching parameter for the fundamental and SH waves ($n_2^{ef}-n_1^{ef}$) reaches a minimum. Note that the intensity of the SH signal in the PBG structure under study, with a number of periods $N=7$ [Fig. 7(c)] is much less then in the ''ideal'' case with $N=20$ [Fig. 2(c)]. This is concerned with the strong absorption of the SH wave in ZnS layers of the real structure, as well as with the different structure thicknesses.

VI. CONCLUSIONS

We have developed a recurrence relation approach to study the efficiency of SF and SH generation in finite one-dimensional PBG structures. We focused our attention on the role of nonphase matching enhancement, that is, the enhancement due to an increase of the energy density of fields near the PBG edges, in the process of nonlinear signal formation, if quasiphase matching interaction takes place. It was shown that the contribution of nonphase matching enhancement is basic, and leads to the growth of the intensity of a quasiphase matching nonlinear signal greater than one order of magnitude. The intensity of the nonlinear signal is weak even if the quasiphase matching condition is fulfilled, but nonphase matching enhancement is absent, if the field frequencies are turned far enough from the PBG edges. We have experimentally demonstrated the nonphase matching enhancement of a SF signal near the condition of quasiphase matching interaction, as well as simultancous SH generation under conditions of nonphase matching enhancement, quasiphase matching interaction, and near dispersive phase matching.

ACKNOWLEDGMENTS

We would like to thank the Université du Littoral for the financial support during the course of these experiments. This work was supported in part by the Russian Foundation for Basic Research (Grant No. 98-02-17544) and BMBF (Grant No. 0081/99 13N7516). The Laboratoire de Physico Chimie de l'Atmosphère participates with the Center d'Etude et de Recherche Lasers et Applications, supported by the Ministère de la Recherche, the Région Nord/Pas de Calais, and the Fond Européen de Développement Economique des Régions. A. P. S. especially acknowledges the support of the Région Nord/Pas de Calais during the course of the experiments.

[1] S.A. Akhmanov and R.V. Khokhlov, *Problems of Nonlinear Optics* (Viniti, Moscow, 1964).
[2] N. Bloembergen, *Nonlinear Optics* (Benjamin, New York, 1965).
[3] V.D. Dmitriev, G.G. Gurzadyan, and D.N. Nikogosyan, *Handbook of Nonlinear Optical Crystals* (Springer-Verlag, Berlin, 1991).
[4] *Photonic Band Gap Materials*, edited by C.M. Soukoulis (Kluwer, Dordrecht, 1996).
[5] E. Yablonovitch, Phys. Rev. Lett. **58**, 2059 (1987).
[6] Z.G. Pinsker, *Dynamical Scattering of X-rays in Crystals*, Springer Series in Solid-State Science Vol. 3 (Springer, Berlin, 1977).
[7] S. John, Phys. Rev. Lett. **58**, 2486 (1987).
[8] S. John and T. Quang, Phys. Rev. A **50**, 1764 (1994).
[9] B.I. Mantsyzov and R.N. Kuz'min, Zh. Éksp. Teor. Fiz. **91**, 65 (1986) [Sov. Phys. JETP **64**, 37 (1986)]; W. Chen and D.L. Mills, Phys. Rev. Lett. **58**, 160 (1987); C. Conti, S. Trillo, and G. Assanto, *ibid.* **78**, 2341 (1997).
[10] V. Berger, Phys. Rev. Lett. **81**, 4136 (1998).
[11] B. Busson, M. Kauranen, C. Nuckolls, T.J. Katz, and A. Persoons, Phys. Rev. Lett. **84**, 79 (2000).
[12] M.M. Fejer, G.A. Magel, D.H. Jundt, and R.L. Byer, IEEE J. Quantum Electron. **28**, 2631 (1992).
[13] J.A. Armstrong, N. Bloembergen, J. Ducuing, and P.S. Pershan, Phys. Rev. **127**, 1918 (1962); N. Bloembergen and A.J. Sievers, Appl. Phys. Lett. **17**, 483 (1970).
[14] A. Yariv and P. Yeh, J. Opt. Soc. Am. **67**, 438 (1977); J. Martorell and R. Corbalan, Opt. Commun. **108**, 319 (1994); J. Martorell, R. Vilaseca, and R. Corbalan, Phys. Rev. A **55**, 4520 (1997).
[15] M. Centini, C. Sibilia, M. Scalora, G. D'Aguanno, M. Bertolotti, M.J. Bloemer, C.M. Bowden, and I. Nefedov, Phys. Rev. E **60**, 4891 (1999).
[16] M. Scalora, M.J. Bloemer, A.S. Manka, J.P. Dowling, C.M. Bowden, R. Viswanathan, and J.W. Haus, Phys. Rev. A **56**, 3166 (1997).
[17] A.V. Balakin, V.A. Bushuev, N.I. Koroteev, B.I. Mantsyzov, I.A. Ozheredov, A.P. Shkurinov, D. Boucher, and P. Masselin, Opt. Lett. **24**, 793 (1999).
[18] A.V. Balakin, V.A. Bushuev, B.I. Mantsyzov, P. Masselin, I.A. Ozheredov, and A.P. Shkurinov, JETP Lett. **70**, 725 (1999).
[19] A.V. Andreev, O.A. Andreeva, A.V. Balakin, D. Boucher, P. Masselin, I.A. Ozheredov, I.R. Prudnikov, and A.P. Shkurinov, Quantum Electron. **29**, 632 (1999).
[20] Y.R. Shen, *The Principles of Nonlinear Optics* (Wiley, New York, 1984).
[21] D.S. Bethune, J. Opt. Soc. Am. B **6**, 910 (1989).
[22] L.G. Parratt, Phys. Rev. **95**, 359 (1954).
[23] S.M. Rytov, Zh. Éksp. Teor. Fiz. **29**, 105 (1956) [Sov. Phys. JETP **2**, 466 (1956)].
[24] A.V. Balakin, D. Boucher, E. Fertein, P. Masselin, A.V. Pakulev, A.Yu. Resniansky, A.P. Shkurinov, and N.I. Koroteev, Opt. Commun. **141**, 343 (1997).
[25] A.P. Shkurinov, N.I. Koroteev, G. Jonusauskas, and C. Rulliere, Chem. Phys. Lett. **223**, 573 (1994).